Electrochemistry of Mesoporous Organosilica of MCM-41 Type Containing 4,4′-Bipyridinium Units: Voltammetric Response and Electrocatalytic Effect on 1,4-Dihydrobenzoquinone Oxidation

Antonio Doménech,*,† Mercedes Alvaro,‡ Belen Ferrer,‡ and Hermenegildo García‡

Departamento de Química Analítica, Universidad de Valencia, Dr. Moliner 50, 46100 Burjasot, Valencia, Spain, and Instituto de Tecnología Química CSIC−UPV, Avenida de los Naranjos s/n, 46022 Valencia, Spain

Received: July 16, 2003; In Final Form: September 10, 2003

The electrochemistry of a novel organic−inorganic material in which 4,4′-bipyridinium units (BP) are covalently attached to the walls of a periodic mesoporous organisilica (PMO) of the MCM-41 type is described. The pristine material (BP@PMO), having its internal space completely filled by the cetyltrimethylammonium structure-directing agent, is almost electrochemically silent. In contrast, the extracted material obtained after removal of the structure-directing agent (BP@PMO-ex) exhibits two reduction peaks at −0.36 and −0.75 V vs AgCl/Ag in contact with aqueous electrolytes. BP@PMO-ex shows a remarkable electrocatalytic effect on the oxidation of 1,4-dihydrobenzoquinone (H_2Q) that is studied by rotating disk voltammetry. At low scan rates the catalytic process is under diffusion/convection control, with a second-order reaction between the surface catalyst and H_2Q acting as a rate-determining step. At high rotation rates the catalytic process becomes independent of the mass transfer, in agreement with the idea that electroactive bipyridinium centers are confined to a boundary zone of the MCM-41 grains.

1. Introduction

The preparation of hybrid organic−inorganic solids in which an organic component is confined in the regular compartmentalized space provided by an inorganic host has attracted considerable attention in past years. From the seminal contributions of Ozin[1] and Terasaki,[2] it is possible to prepare a strictly regular periodic mesoporous organosilica (PMO) of the MCM-41 type in which the organic groups form part of the silica walls by synthesizing an organic derivative having two terminal siloxane groups. The synthesis of such PMO materials requires the use of cetyltrimethylammonium (CTMA) as structure-directing agent, and the resulting as-synthesized solid has an internal space completely filled by the structure-directing (or template) agent. According to the accepted formation mechanism of MCM-41, crystallization of the silicate walls occurs surrounding the self-assembled surfactant, accomplishing the maximum possible close packing.

The synthesis of PMO of the MCM-41 type in which an organic guest occupies framework positions in the walls rather than in the empty voids of the hexagonal channels of the MCM-41 host has been recently described.[3−5] In this context, we have previously reported a new PMO in which 4,4′-bipyridinium units are covalently inserted in MCM-41 walls, the template being subsequently extracted from the solid without removing covalently grafted viologen ions.[6] This novel material, labeled here as BP@PMO-ex, combines the properties of the inorganic MCM-41 substrate with the strong electron acceptor character of viologen units.[7] This material provides unusual abilities for stabilizing viologen radical cations through thermal and photochemical activation.[6] The as-synthesized material, BP@PMO, is characterized by having virtually no internal empty space and the viologen units covalently attached to the walls uniformly distributed and without possibility of diffusion.

The purpose of the current work is to describe the electrochemistry of this novel material, attempting to verify the possibility of an efficient electrochemical generation of viologen radical cations, subsequently acting as active species in catalytic redox cycles.

Additionally, this electrochemistry may be of interest with regard to the controversy existing on the behavior of electroactive species associated with microporous solids.[8,9] In particular, the electrochemistry of methyl viologen associated with zeolite Y in contact with aqueous electrolytes has been interpreted differently.[10−15] Thus, Calzaferri et al. described the voltammetry of methyl viologen exchanged zeolite Y deposited as a monograin layer on glassy carbon electrodes in terms of an intrazeolite charge transfer,[13] whereas Hui and Baker described such electrochemistry in terms of an extrazeolite redox process rate limited by ion-exchange kinetics.[14,15]

Aimed at addressing this matter, the electrochemistry of pristine viologen-containing MCM-41 (BP@PMO) and that of the extracted material obtained after removal of the structure-directing cetyltrimethylammonium template (BP@PMO-ex) have been studied. PMOs can be freed from the surfactant and the pores emptied by exhaustive solid−liquid extraction using acidic ethanol/*n*-heptane mixtures. Spectroscopic data indicate that any viologen not covalently attached due to the imperfection of the synthesis has been removed during the extraction. Accordingly, it is possible to have at hand two related BP@PMO and BP@PMO-ex materials in which bipyridinium units are uniformly distributed and covalently attached to the walls of MCM-41, but sharply differing in the accessibility of internal channels.

Since electron-transfer processes involving electroactive species associated with microporous materials involve the ingress/issue of electrolyte countercations to maintain charge

* Corresponding author. E-mail: antonio.domenech@uv.es.
† Universidad de Valencia.
‡ Instituto de Tecnología Química CSIC−UPV.

10.1021/jp030852w CCC: $25.00
Published on Web 10/23/2003

neutrality,[16,17] the presence or absence of the template emptying the voids of MCM-41 can provide significant differences between the electrochemical responses of BP@PMO and BP@PMO-ex.

To study the electrochemical response of such materials, polymer film electrodes (PFEs)[18,19] and paraffin-impregnated graphite electrodes (PIGEs)[20] have been used in contact with aqueous NaCl solutions. Square wave voltammetry (SQWV) has been used in addition to linear potential scan (LSV) and cyclic (CV) voltammetries because of its inherently high analytical sensitivity and its immunity to capacitive effects.[21] This last property is of particular interest in view of the insulator characteristics of the studied materials, thus promoting undesired charging effects in electrochemical experiments.

Attempting to explore the capabilities of PMOs for promoting electron-transfer reactions, the electrocatalytic effect of BP@PMO and BP@PMO-ex on the oxidation of 1,4-dihydrobenzoquinone (H_2Q) in aqueous media has been studied. The electrochemistry of quinone/hydroquinone systems has been widely studied, consisting of coupled proton-transfer/electron-transfer processes.[22−27] In view of the recognized electron acceptor ability of methyl viologens,[28] BP@PMO and BP@PMO-ex can exhibit a catalytic effect on the oxidation of hydroquinones that could be related to the adsorption capacity and redox properties of such materials.

2. Experimental Section

2.1. Preparation and Characterization of Materials. The preparation of the solid of MCM-41 type incorporating 4,4′-bipyridinium units was accomplished following the general methodology described for similar materials having methylene groups covalently linked to the walls.[4] The procedure starts from the attachment of trimethoxysilylpropyl groups to the nitrogen atoms of 4,4′-bipyridine by nucleophile substitution. The silylated viologen precursor is then used in combination with tetraethoxysilane (TEOS) in the synthesis of the BP@PMO using cetyltrimethylammonium bromide as the structure-directing agent, as previously described.[6]

Thermogravimetric analysis coupled with differential scanning calorimetry under air stream shows three peaks: one from 150 to 250 °C corresponds to 30 wt % and is attributed to the decomposition/desorption of the cetyltrimethylammonium bromide. The second peak occurs between 250 and 450 °C and varies depending on the BP content, up to a maximum of 11.5 wt % for the sample with the highest BP content. This peak most probably corresponds to the degradation of BP simultaneously with a residual amount of cetyltrimethylammonium. A final tail (ca. 4 wt %) from 450 to 900 °C could be due to loss of H_2O by silanol condensation and formation of silanoxy bridges. Characterization of the materials by X-ray diffraction and FT-IR data has been already reported (see Supporting Information).[6]

2.2. Extraction Procedure for the Removal of the Cetyltrimethylammonium Bromide. The periodic mesoporous organosilicas were extracted in two steps, following the procedure reported in the literature for related MCM-41 materials. In the first step the solid was stirred at 70 °C with an ethanol solution of 0.05 M H_2SO_4 for 1 h. The solid:liquid weight ratio was 1:50. After this time, the suspension was cooled and the solid was recovered by filtration, washed copiously with ethanol, and dried in an oven at 100 °C. In a second extraction, the resultant solid was magnetically stirred overnight at 90 °C in a ethanol: *n*-heptane (48:52)/0.15 N HCl mixture. Then the solid was filtered, washed thoroughly with ethanol:*n*-heptane (48:52) mixture, and dried in an oven at 100 °C.

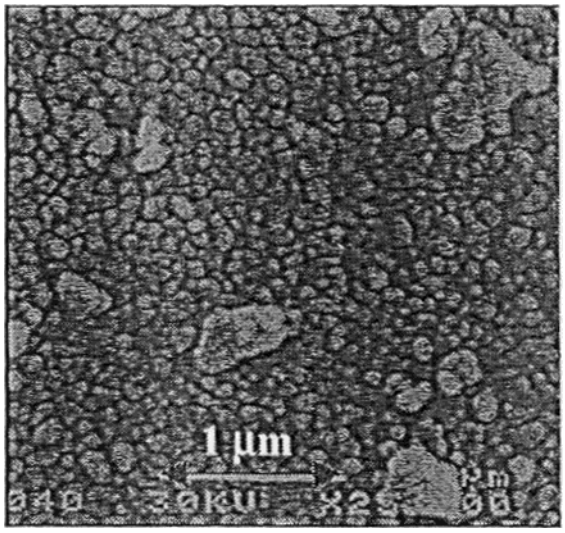

Figure 1. Scanning electron microscopy (SEM) photograph of as-synthesized BP@PMO.

Surface area determined according to the BET algorithm from the isothermal gas adsorption of the BP@PMO sample after cetyltrimethylammonium removal gives 930 $m^2 \cdot g^{-1}$, with a mononodal pore size distribution centered at 3.8 nm and a total pore volume of 0.88 $mL \cdot g^{-1}$.

These values are within the expected range for a typical MCM-41.[29] Figure 1 shows a scanning electron microscopy (SEM) image of the as-synthesized BP@PMO. The solid contains a fairly uniform distribution of almost spherical particles of about 0.1 μm diameter partly forming large aggregates. The morphology of the particles remains unaltered after extraction. Combustion chemical C and N analysis of the BP@PMO-ex indicates that the viologen content is 0.2×10^{-3} mol/g.

2.3. Modified Electrode Preparation. Commercially available Paraloid B72, an ethyl acrylate (70%)−methyl acrylate (30%) copolymer (P[EMA/MA]) was selected for polymer film electrode preparation because of its mechanical stability and ability to form porous films able to adhere the zeolite microparticles to the electrode surface.

Polymer film sample-modified electrodes were prepared, as previously described,[18,19] by transferring a few microliters (typically 50 μL) of a dispersion of the solid (10 mg) in acetone (5 mL) to the surface of a freshly polished glassy carbon electrode and allowing the coating to dry in air. After the electrode surface was air-dried, one drop of a solution of the acrylic resin (1%) in acetone was added and the modified electrode was air-dried. The coatings examined contained 0.2−1.5 mg/cm^2 BP@PMO or BP@PMO-ex.

To facilitate the direct contact between the zeolite particles and the substrate electrode, which is a crucial aspect for studying the electrochemistry of zeolite-associated species,[8−11] paraffin-impregnated graphite electrodes were also used. These electrodes, developed by Scholz et al.,[20] have been extensively used in past years for studying the electrochemical behavior of solid materials. Cylindrical rods of 5 mm diameter graphite impregnated under vacuum by paraffin were prepared as described in ref 20.

To prepare modified paraffin-impregnated graphite electrodes, 1−2 mg of zeolite was placed on a glazed porcelain tile, forming a spot of finely distributed material. Then the lower end of the graphite electrode was gently rubbed over that spot of sample and finally cleaned with a tissue paper to remove ill-adhered particles.

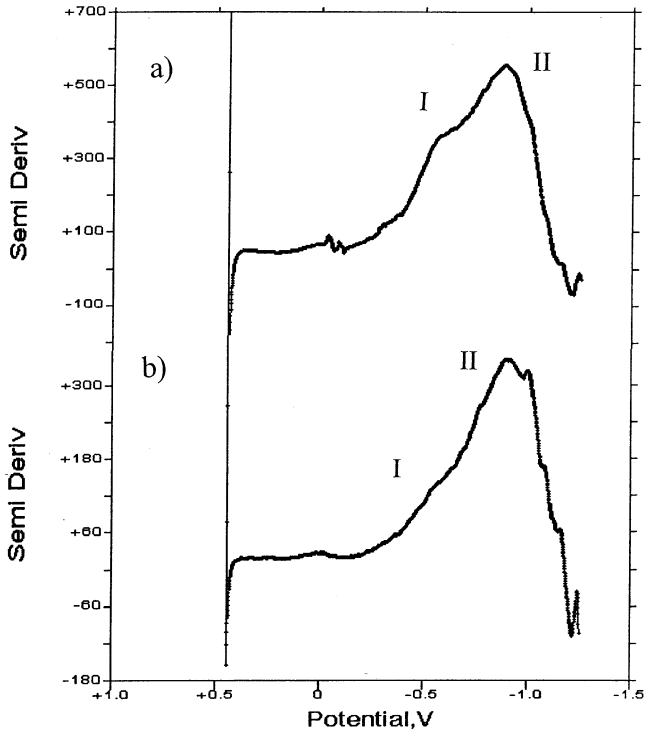

Figure 2. LSVs (semiderivative convolution) of PFEs modified by (a) BP@PMO-ex and (b) BP@PMO immersed in 0.10 M NaCl. Potential scan initiated at +0.45 V just after the immersion of the modified electrodes in the electrolyte solution. Potential scan rate 50 mV/s.

2.4. Instrumentation and Procedures. Linear potential scan (LSVs), cyclic voltammograms (CVs), and square wave voltammograms (SQWVs) were performed with BAS CV50W and CH 420I equipment. A standard three-electrode arrangement was used with a platinum auxiliary electrode and a AgCl (3 M NaCl)/Ag reference electrode (SCE) in a thermostated cell. A glassy carbon (BAS MF 2012, geometrical area 0.071 cm^2) working electrode was used for PFE preparation. Rotating disk voltammetry was carried out with a Metrohm 628-10 assembly.

Experiments were conducted in aqueous media using NaCl (Merck) as a supporting electrolyte. For catalytic experiments, solutions of 1,4-dihydrobenzoquinone (Aldrich) in concentrations ranging from 0.02 to 40 mM were used. Experiments in H_2Q plus NaCl solutions were performed at PIGEs modified by BP@PMO and BP@PMO-ex materials after 10 min of contact of the modified electrode with the quiescent solution. Unless stated, 1 mg of modifier was used routinely. All electrochemical measurements were performed in well-deaerated solutions under an atmosphere of argon.

3. Results and Discussion

3.1. Electrochemistry of BP@PMO and BP@PMO-ex. Figure 2a shows the cathodic LSV of a BP@PMO-ex modified PFE recorded just after immersion in 0.10 M NaCl. An ill-defined response is obtained that, after semiderivative convolution, reveals the presence of two reduction processes at −0.7 (I) and −1.0 V (II). The voltammogram of the as-synthesized material, BP@PMO (see Figure 2b), consists of weaker signals, peak II being enhanced at the expense of peak I.

The voltammetric record, however, varies significantly upon repetitive scanning the potential and/or prolonging the time of contact between the modified electrode and the electrolyte solution. Increased peak resolution was obtained using sample-modified PIGEs and SQWV as a detection mode. This can be seen in Figure 3, in which the SQWVs of (a) BP@PMO-ex and (b) BP@PMO, recorded after 10 repeated scans, are shown. For BP@PMO-ex, two well-defined peaks appear at −0.34 (III) and −0.56 V (IV), followed by ill-defined shoulders near−0.9 and −1.6 V, and preceded by a weak peak near −0.14 V. For BP@PMO, only a peak at −0.12 V is clearly recorded. This peak is attributable to any background signal as judged by comparison with the voltammograms of pristine, viologen-absent, PMO materials. The weak shoulder near−0.9 V appears to correspond with peak II recorded in first scan voltammograms, whereas the shoulder at more negative potentials (−1.6 V) can tentatively be ascribed to the proton-assisted reduction of neutral BP units in solution phase, following the general scheme observed for the electrochemical reduction of aromatic compounds.[27]

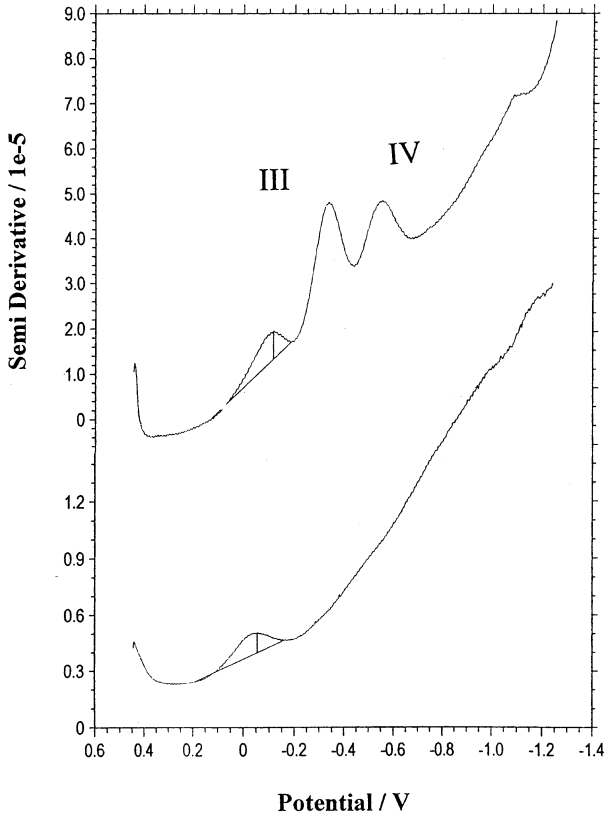

Figure 3. SQWVs recorded after 10 repeated scans of PIGEs modified by (a, top curve) BP@PMO-ex and (b, bottom curve) BP@PMO immersed in 0.10 M NaCl. Potential scan initiated at +0.45 V in the negative direction. Potential step increment 4 mV; square wave amplitude 25 mV; frequency 15 Hz.

The voltammetric response of BP@PMO-ex and BP@PMO immediately after immersion in the electrolyte solution is in principle similar to that reported for bipyridinium dications in aqueous solution and associated with zeolite Y.[15−17] In neutral aqueous media, the reduction of BP^{2+} occurs via two reversible one-electron reduction steps near−0.7 and −1.0 V vs SCE which can be represented as

$$BP^{2+} + e^- = BP^{\bullet +} \quad (1)$$

$$BP^{\bullet +} + e^- = BP^0 \quad (2)$$

The neutral BP^0 product comproportionates with the parent BP^{2+} within the second reduction process

$$BP^{2+} + BP^0 = 2BP^{\bullet +} \quad (3)$$

to yield $BP^{\bullet+}$, which can be further reduced to BP^0. Accordingly, the second voltammetric wave is enhanced with respect to the first.[31]

The enhancement of that second voltammetric wave was also observed for zeolite-associated methyl viologen, the relative height of the waves corresponding to the first and second one-electron-transfer processes being dependent on the electrolyte cation. The observed electrochemistry was interpreted in terms of the occurrence of an intrazeolite charge transfer by Calzaferri et al.,[13] whereas Hui and Baker[14,15] described such electrochemistry in terms of an extrazeolite redox process rate limited by ion-exchange kinetics. These authors obtained an additional anodic peak at a potential intermediate between those of the "ordinary" one-electron peaks which is attributed to the oxidation of zero-valent methyl viologen deposited on the electrode surface.

The response of BP@PMO-ex recorded after repeated scans is, however, remarkably different from those of BP^{2+} in aqueous solution and associated with zeolite Y. Thus, (i) the reduction processes III and IV of BP@PMO-ex occur at potentials significantly less negative than those reported for BP^{2+} in solution and associated with zeolite Y; (ii) there is no enhancement of peak IV at the expense of peak III, i.e., no significant comproportionation effects in BP@PMO-ex systems; and (iii) no traces of adsorption-like oxidation processes were detected in such systems.

These results can be rationalized on assuming that the response of BP@PMO is due to "external" viologen units leached from the surface of the material, whereas the electrochemistry of BP@PMO-ex results from the superposition of the response of such external viologen units and that of boundary-associated ones. Accordingly, the initial response (see Figure 2) of BP@PMO and BP@PMO-ex is dominated by such "external" bipyridinium ions, with peak potentials at -0.7 (I) and -1.0 V (II).

Upon repetitive cycling of the potential scan, the response of BP@PMO largely decays whereas that of BP@PMO-ex changes remarkably. This last consists of two cathodic processes at -0.34 (III) and -0.56 V (IV) (see Figure 3) that can be described in terms of the reduction of bipyridinium units which remain associated, to a some extent, with the MCM-41 boundary. Then, the electrode processes are presumably associated with the ingress of charge-balancing electrolyte countercations on the MCM-41 pore/channel system, as described for zeolite-associated electroactive molecules.[16,17] The corresponding electrochemical processes can be represented as

$$BP^{2+}(b) + M^+ + e^- = BP^{\bullet+}(b) + M^+(b) \quad (4)$$

$$BP^{\bullet+}(b) + M^+ + e^- = BP^0 + M^+(b) \quad (5)$$

where (b) represents the PMO boundary region and M^+ the electrolyte cations.

Since that response involves the ingress of electrolyte cations in the MCM-41 matrix, it must be favored by prolonging the contact time between the solid and the electrolyte solution. By contrast, the response of the external bipyridinium units must decrease with time as a result of the diffusion of such units to the bulk of the solution. Accordingly, the voltammetry in the initial scans (Figure 2) reflects the superposition of electrode processes for free and boundary-associated species. After several scans (Figure 3), the observed voltammograms must provide mainly the response due to boundary-associated molecules.

The apparently dual response recorded for BP@PMO-ex is in principle consistent with the observed variation of the peak

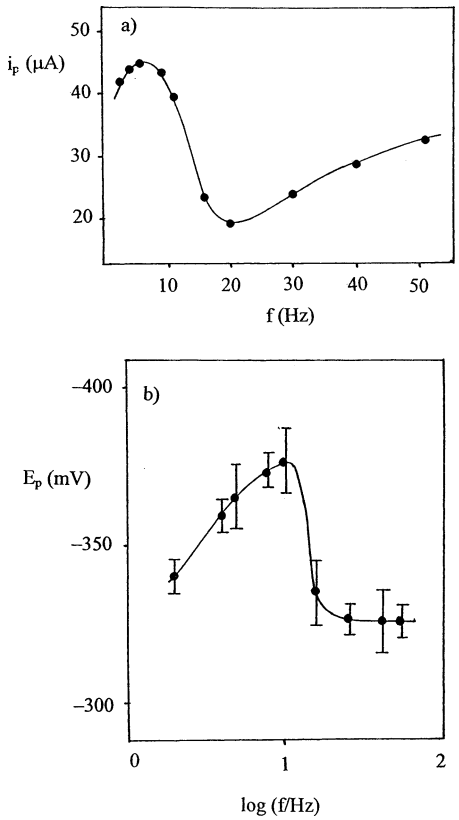

Figure 4. SQWVs recorded after 10 min of contact between a PIGE modified by BP@PMO-ex and a 0.10 M NaCl aqueous solution. (a) Variation of peak current as a function of square wave frequency; (b) variation of peak potential on log *f*. Potential step increment 4 mV; square wave amplitude 25 mV.

potential, E_p, and peak current, i_p, of SQWVs with the frequency *f*. As shown in Figure 4a, after 10 min of contact time between the electrode and the solution, the peak current increases initially as the frequency increases until a maximum is reached near 5 Hz. For *f* values larger than 5 Hz, the peak current decreases on increasing frequency until for *f* values near 20 Hz the peak current again increases. In this last region of the i_p vs *f* graph, the peak current becomes proportional to $f^{1/2}$, as expected for an "ordinary" diffusion-controlled electron-transfer process.

Similarly, as shown in Figure 4b, peak potentials recorded at frequencies below 10 Hz are negatively shifted on increasing *f*. At larger frequencies, however, the values of E_p increase abruptly and remain essentially *f* independent.

These data differ from those obtained at zeolite-associated methyl viologen for which peak currents monotonically increasing on increasing the potential scan rate were obtained.[13,14] In fact, for an electrode process controlled by the diffusion of "external" ions or by the diffusion of electrolyte countercations on the zeolite system, a growth of the peak current on the potential scan rate has to be expected.[14] This corresponds in SQWV to a proportionality between i_p and $f^{1/2}$ or eventually, in the case of a thin-layer behavior,[19] to a proportionality between i_p and *f*.

The unusual variation of i_p and E_p with *f* observed for BP@PMO-ex can be interpreted assuming that there is a limiting depth for which BP^{2+} units are electrochemically accessible. Accordingly, there is a compromise between the diffusion of electrolyte countercations through the MCM-41 channels and the rate of electron transfer on/to boundary-associated BP^{2+}.

On first examination, the presence of peak current drops can be associated with preceding reactions, as described for SQWV

of reactants in solution.[34] Since bipyridinium units are covalently attached to the walls of MCM-41 and form charge-transfer complexes with accompanying halide ions,[6,35] reduction processes may involve prior breaking of covalent bonds with the silicate framework and/or removing halide coordination. Accordingly, the reduction of bipyridinium units would be described in terms of the reduction of "free" BP^{2+} units preceded by the breaking of their linkages with the silicate framework.

The observed variation of the peak current of BP@PMO-ex on the square wave frequency, however, differs from those theoretically predicted for preceding reactions, for which the peak current decreases monotonically as the frequency increases. In fact, the experimental response of BP@PMO-ex parallels that described for SQWV at thin mercury film electrodes.[36] Here, the response at relatively high frequencies is close to that of reversible processes with unrestricted planar diffusion, whereas for low frequencies no concentration gradients exist in the film on the time scale of the potential step perturbation. In both cases the peak current is proportional to the square root of the frequency and the peak potential becomes *f* independent. For intermediate frequencies, however, the diffusion length in solution at the time of current measurements becomes larger than the film thickness, with the flux of the oxidized form at the electrode surface decreasing sharply with decreasing frequency. As a result, the peak current increases dramatically while the peak potential shifts slightly toward more negative values.[36]

The total charge uptake measured from the area of the current peak in LSVs performed at 5 mV/s provided values of 8 and 21 μC/g for BP@PMO and BP@PMO-ex, respectively. This difference clearly indicates that after removal of the surfactant some more viologen located not on the external surface became accessible; the response of the extracted material was accordingly higher than those of the as-synthesized one. With these data and considering a simplified model in which the sample is formed by spherical particles having homogeneously distributed viologen, an estimation of the depth of penetration in the particle during the electrochemical measurements can be made. In this simplified model the difference between the charge uptake of BP@PMO-ex and BP@PMO must correspond to the internal viologen located in a spherical crown whose radius would be 0.050 μm; i.e., the penetration inside the particle was calculated as only 0.04% of the particle size. This result is in agreement with the literature concerning the electrochemistry of zeolite-associated species: following Bessel and Rolison, electroactive molecules must be external to the zeolite or located in the more external boundary zone of the same.[30] All these considerations are consistent with prior results on the electrochemistry of zeolite Y associated $Mn(salen)N_3$ (salen = *trans*-(*R*,*R*)-1,2-bis(salicylideneamino)cyclohexane),[18] and zeolite Y associated 2,4,6-triphenylthiopyrylium ion.[19] In agreement with these ideas, it has been reported that interfacial electron transfer to zeolite-associated MV^{2+} from various carbonylmanganate donors occurs only in the zeolite periphery.[31]

3.2. Electrocatalysis of 1,4-Dihydrobenzoquinone Oxidation. The electrocatalytic effect of BP@PMO and BP@PMO-ex on the electrochemical oxidation of 1,4-dihydrobenzoquinone (H_2Q) has been studied upon attachment of such probes to PIGEs. In Figure 5 the cyclic voltammetric response of a bare PIGE and such modified electrodes immersed in a 1.2 mM H_2Q plus 0.10 M NaCl solution at pH 5.2 are shown.

As can be seen in Figure 5a, at an unmodified electrode, two overlapped anodic peaks appear near +0.58 and +0.76 V, followed, in the subsequent cathodic scan, by reduction peaks at +0.05 and −0.14 V. This response is in agreement with the

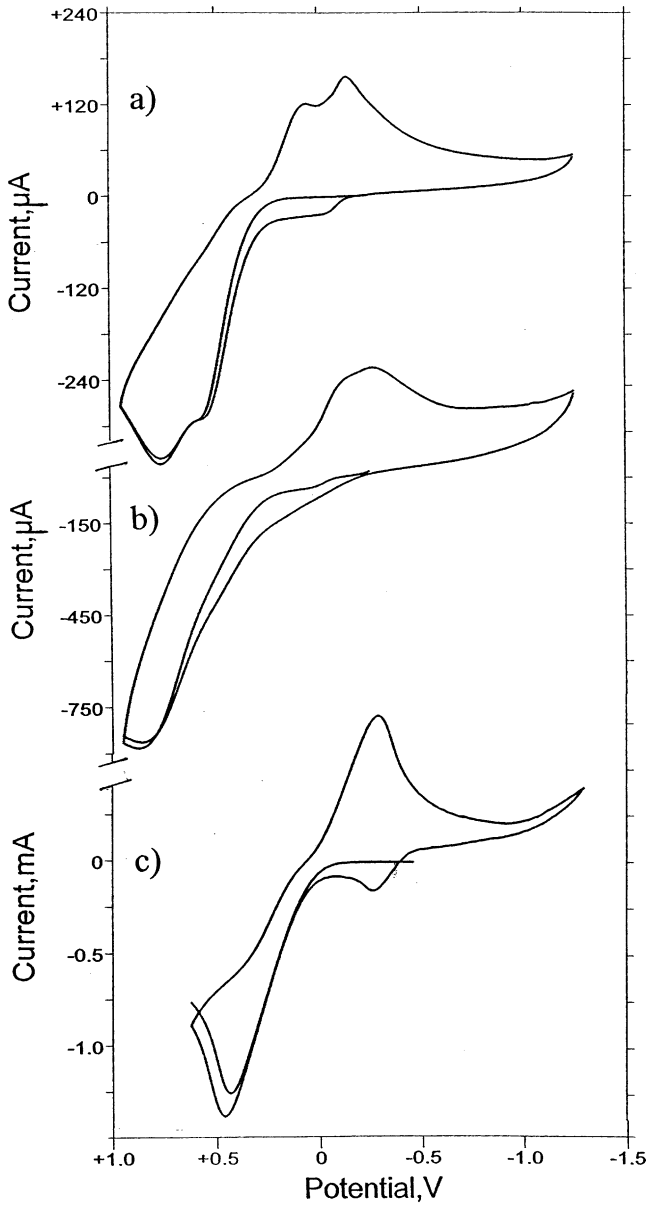

Figure 5. CVs of (a) unmodified, (b) BP@PMO modified, and (c) BP@PMO-ex modified PIGEs immersed in 1.20 mM H_2Q + 0.10 M NaCl, pH 5.20. Potential scan rate 100 mV/s.

proposed models for quinone/hydroquinone systems. In particular, at pH values between 2 and 7, the reduction of benzoquinone takes place through a electron/proton/proton/electron transfer sequence (ECCE scheme).[22,23] Assuming a similar scheme for the inverse processes, the oxidation of H_2Q can be represented as

$$H_2Q \xrightarrow{-e^-} H_2Q^{\bullet +} \xrightarrow{-H^+} HQ^{\bullet} \xrightarrow{-H^+} Q^{\bullet -} \xrightarrow{-e^-} Q \qquad (6)$$

This scheme, however, may be mediated by solution-electron-transfer (SET) reactions, studied in detail by Hawley and Feldberg[37,38] and by Savéant and co-workers.[39−41] Thus, the neutral radical HQ•, is capable of being reduced by the anion radical itself:[29]

$$HQ^{\bullet} + Q^{\bullet -} = HQ^- + Q \qquad (7)$$

At a BP@PMO-modified electrode (Figure 5b), the CV response is quite similar, but the peak current is 2-fold that recorded at the unmodified electrode. For a PIGE modified with

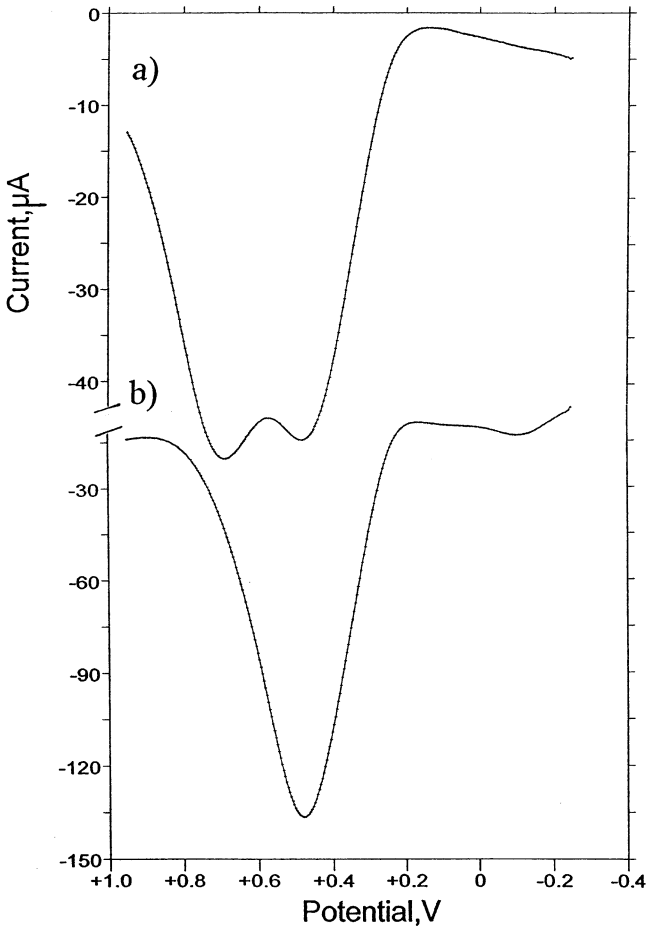

Figure 6. SQWVs at (a) BP@PMO modified and (b) BP@PMO-ex modified PIGEs immersed in 1.00 mM H_2Q + 0.10 M NaCl; pH 4.70. Potential step increment 4 mV; square wave amplitude 25 mV; frequency 2 Hz.

BP@PMO-ex, only the first anodic peak and the first cathodic peak apparently remain while the peak current is significantly (10−15 times) enhanced; additionally, in the second and subsequent scans, a new anodic peak appears at ca. 0 V (Figure 5c). SQWVs of H_2Q solutions at BP@PMO-modified electrodes exhibit two overlapped peaks, whereas those recorded at BP@PMO-ex present an unique peak as can be seen in Figure 6.

The catalytic currents are enhanced on increasing the amount of BP@PMO-ex deposited on the graphite electrode between 0.2 and 2 mg of the material. The following data refer to surface densities of 1.3 mg/cm^2 of BP@PMO-ex.

For both BP@PMO and BP@PMO-ex modified electrodes, the peak potential for the oxidation of H_2Q is shifted toward more positive values on increasing the potential scan rate, υ, in CVs and the frequency in SQWVs. Plots of CV peak potential, E_p, vs log υ were linear, as well as plots of E_p vs f in SQWVs, as expected for irreversible electrocatalytic systems.[42]

The net anodic peak current in LSVs increased in general on increasing the potential scan rate. Rotating disk voltammetry at modified electrodes immersed in solutions of H_2Q yield typical S-shaped current/potential graphs, as depicted in the inset of Figure 7. At rotation rates (ω) below 800 rpm, a linear dependence of the limiting currents, i_L, on the square root of the rotation rate was obtained (see Figure 7); however, for larger ω values the limiting currents remained almost constant upon variations in the electrode rotation rate. This is illustrated in Koutecky−Levich plots (the reciprocal of the limiting current, i_L^{-1}, vs the reciprocal of the square root of the rotation rate,

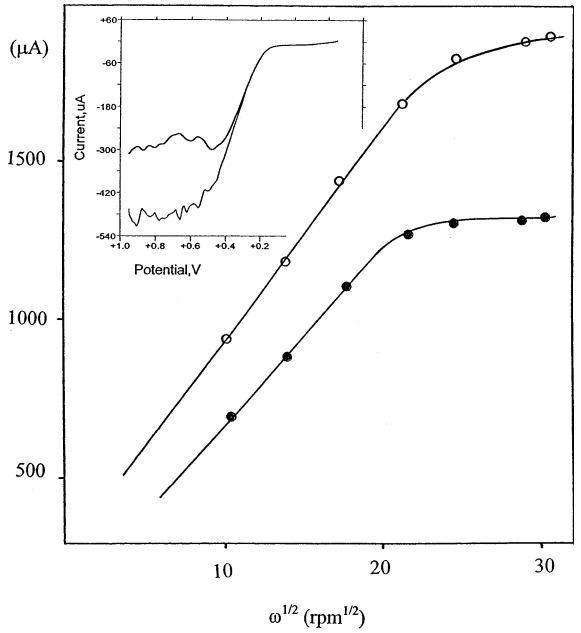

Figure 7. Levich plots of limiting current vs $\omega^{1/2}$ for LSVs performed at rotating BP@PMO-ex modified PIGEs immersed in 1.00 mM H_2Q + 0.10 M NaCl at pH 5.20 (○) and 4.80 (●). Potential scan rate 100 mV/s. Inset: LSVs obtained at pH 5.00 in 0.20 mM H_2Q + 0.10 M NaCl using rotation rates of 200 and 400 rpm.

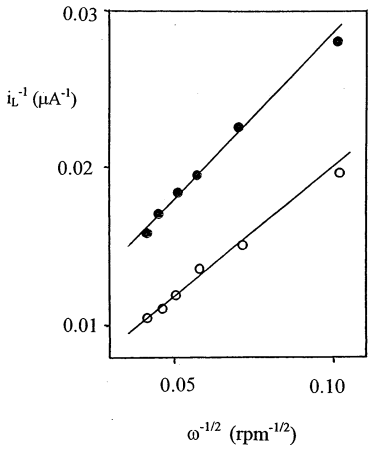

Figure 8. Koutecky−Levich plots of i_L^{-1} vs $\omega^{-1/2}$ in LSVs (υ = 100 mV/s) at rotating disk modified electrodes in the region of relatively low rotation rates. ○, BP@PMO-ex; ●, BP@PMO in 4.10 mM H_2Q + 0.10 M NaCl.

$\omega^{-1/2}$) depicted in Figure 8. In agreement with the theory of mediated electrocatalysis,[43] one can conclude that there is a transition from a diffusion/convection controlled mechanism to a process in which the rate of mass transfer does not affect the electrode response.

The response at low rotation rates can be interpreted in terms of the occurrence of a relatively slow chemical reaction between the analyte and the bipyridinium catalytic sites which represents the rate-determining step in the overall electrode process. Here, the reciprocal of the intercept of the Koutecky−Levich plots defines a potential-independent kinetic current, i_k, which verifies[43]

$$i_k = nFAk\Gamma c \tag{8}$$

where k represents a second-order rate constant, Γ is the surface concentration of catalyst present on the electrode surface, c denotes the concentration of hydroquinone in the solution, and the other symbols have their customary meaning.

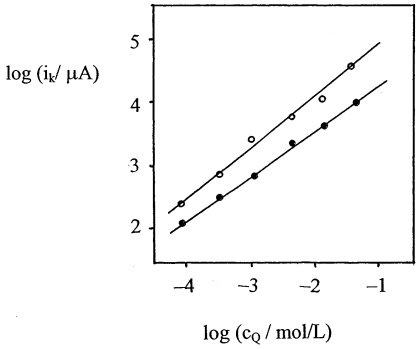

Figure 9. Plots of log i_k, determined from intercept of Koutecky−Levich plots, vs logarithm of hydroquinone concentration for BP@PMO-ex modified electrodes. ○, pH 5.3; ●, pH 4.2.

As can be seen in Figure 9, the representations of log i_k vs log c at pH 5.0 and 4.0 provide straight lines whose slope is close to unity, thus suggesting that the current-limiting reaction is first-order in hydroquinone. From the slope of such representations one can obtain the value of the second-order rate constant, k, for the reaction between hydroquinone and the catalyst, as described in the literature.[43,44] On using the effective amount of bipyridinium ions determined from prior voltammetric data (2.2×10^{-10} mol/cm^2), the value of k is 1.6×10^4 L/(mol s), similar to those values reported by Lei and Anson for the catalysis of oxygen reduction by metal complexes adsorbed on graphite electrodes.[44]

At relatively high rotation rates, however, the plateau currents become essentially constant (see Levich plots in Figure 7). This kinetic situation can correspond to a reaction which is occurring throughout the layer of modifier and is controlled by the kinetics of that cross-reaction, as described by Doherty and Vos,[45] for the electrocatalytic reduction of nitrite at electrodes modified by redox polymers. For BP@PMO-ex, this situation can be described in terms of the kinetic control exerted by the diffusion of hydroquinone through the solid material to react with surface-confined bipyridinium units.

The electrocatalytic effect exerted by BP@PMO-ex can be ascribed to the combination of the electron-acceptor ability of bipyridinium units and confinement effects due to the attachment to the PMO matrix. On the basis of the previous considerations, the electrocatalytic effect of BP@PMO-ex must result from the superposition of the effect associated with more external bipyridinium centers (thus explaining the weak catalytic effect of the as-synthesized BP@PMO material) and that due to boundary-associated ones.

Interestingly, BP@PMO and BP@PMO-ex display different variations of their catalytic effects on the pH. As shown in Figure 10, for BP@PMO the catalytic peak current for H_2Q oxidation decreases monotonically on increasing the pH. For BP@PMO, however, the catalytic current increases on increasing the pH until it reaches a maximum near pH 5.5, further decreasing rapidly on increasing the pH.

Since the catalytic effect associated with BP@PMO consists essentially of an enhancement of the second anodic peak for H_2Q oxidation, the catalytic effect can tentatively be associated with a redox reaction in solution phase between bipyridinium ions and any intermediate species resulting from the initial electron transfer of H_2Q (see eq 6). Since the catalytic effect decreases monotonically on increasing the pH, a plausible rate-determining reaction is

$$Q^{\bullet -} + BP^{2+} = Q + BP^{\bullet +} \qquad (9)$$

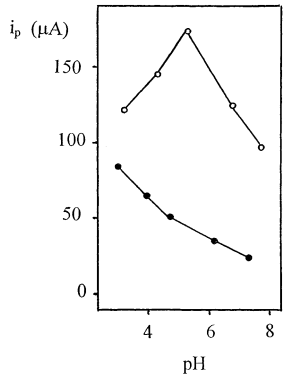

Figure 10. pH dependence of peak current recorded in LSVs of BP@PMO-ex modified (○) and BP@PMO (●) modified electrodes immersed in 0.33 mM H_2Q + 0.10 M NaCl. Potential scan rate 100 mV/s.

SCHEME 1: Possible Catalytic Process for Oxidation of H_2Q Mediated by BP@PMO-ex

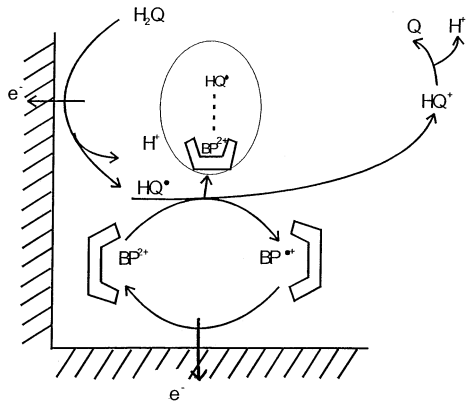

With regard to the electrocatalysis by BP@PMO-ex, it appears reasonable to expect that a different catalytic scheme is operative. This is supported by the fact that (i) catalytic currents obtained with BP@PMO-ex are higher than those recorded with BP@PMO and (ii) the voltammograms recorded at BP@PMO-ex electrodes in H_2Q solutions (see Figure 5) exhibit only the first oxidation peak. This last feature can result from a drastic lowering of the electrode potential of the second electron-transfer step, thus merging the second wave with the first one to give an apparently unique two-electron process.

A possible scheme may involve the formation of a surface adduct between the bipyridinium units and any intermediate semiquinone form resulting from the first electron-transfer step (see eq 6), further yielding a rapid dissociation generating the quinone and the bipyridinium radical cation:

$$BP^{2+}(b) + HQ^\bullet = [BP\cdots HQ](b) = BP^{\bullet +}(b) + Q + H^+ \qquad (10)$$

The rate constant for this second-order reaction is that previously calculated. A possible catalytic cycle is depicted in Scheme 1. In a first stage the hydroquinone is oxidized to $HQ^\bullet$ through an one-electron/one-proton process corresponding to the initial steps described in eq 6. It is assumed that $HQ^\bullet$ forms a surface complex with PMO-associated BP^{2+} which undergoes an internal electron-transfer process yielding HQ^+ and PMO-associated $BP^{\bullet +}$. At the operating electrode potentials, the bipyridinium radical cation must be electrochemically oxidized, thus regenerating the parent PMO-associated BP^{2+}.

These considerations are consistent with the observed variation of the catalytic peak current for H_2Q oxidation with the

pH. As depicted in Figure 10, for BP@PMO the catalytic effect decreases on increasing the pH, in agreement with the expected stabilization of the first $HQ^{\bullet+}$ intermediate in the reaction sequence represented by eq 6. By contrast, for BP@PMO-ex, the catalytic effect reaches a maximum near pH 5.5. This may result from a compromise between the stabilization of $HQ^{\bullet+}$ and, subsequently, $HQ^{\bullet}$, favored at low pHs, and the proton loss accompanying the conjectured rate-determining step, represented by eq 8, favored at high pH values.

4. Final Considerations

The electrochemical response of regular mesoporous organosilica of the MCM-41 type containing bipyridinium units covalently attached differs significantly for as-synthesized material, BP@PMO, having the internal space filled by template molecules, and the extracted probe, BP@PMO-ex, in where the channels have been devoid of such template. Upon repetitive voltammetry, BP@PMO becomes electrochemically silent while BP@PMO-ex exhibits two well-defined reduction peaks at potentials ca. 300 mV less negative than those reported for the reduction of bipyridinium ions in aqueous solution or associated with zeolite Y in contact with aqueous electrolytes.

The square wave voltammetric behavior of BP@PMO-ex can be described in terms of the superposition of the response of external bipyridinium ions and that of boundary-associated ones. The electrochemical response is confined to a shallow boundary zone of the grains of the material. Accordingly, at low frequencies/potential scan rates the diffusion of electrolyte countercations acts as a rate-determining step, whereas at relatively high frequencies/scan rates a thin film-like response is obtained.

BP@PMO-ex exhibits a significant catalytic effect on the electrochemical oxidation of hydroquinone in aqueous ($3 < pH < 8$) media. Upon examination at rotating disk electrodes, two different kinetic regimes are detected for that mediated electrocatalysis: at low rotation rates an "ordinary" diffusion/convection controlled response is obtained, whereas at high rotation rates the catalytic process becomes independent of mass transfer. Electrochemical data are consistent with the occurrence of a second-order reaction between the BP@PMO-ex and the analyte mediated by the diffusion of hydroquinone forms through the solution phase and their ingress into the PMO boundary. This catalytic behavior is consistent with the idea that electroactive bipyridinium centers are confined to a boundary zone of the MCM-41 grains.

Supporting Information Available: Pictorial representation of PMO channels; characterization of PMO materials by X-ray diffraction and FT-IR data. This material is available free of charge via the Internet at http://pubs.acs.org.

References and Notes

(1) MacLachlan, M. J.; Asefa, T.; Ozin, G. A. *Chem. Eur. J.* **2000**, *6*, 2507.
(2) Inagaki, S.; Guan, S.; Ohsuna, T.; Terasaki, O. *Nature* **2002**, *416*, 304.
(3) Inagaki, S.; Guan, S.; Fukushima, Y.; Oshuna, T.; Terasaki, O. *J. Am. Chem. Soc.* **1999**, *121*, 9611.
(4) Melde, B. J.; Holland, B. T.; Blandford, D. F.; Stein, A. *Chem. Mater.* **1999**, *11*, 3302.
(5) Yoshina-Ishiii, C.; Asefa, T.; Coombs, N.; MacLachlan, M. J.; Ozin, G. A. *Chem. Commun.* **1999**, 2539.
(6) Alvaro, M.; Ferer, B.; Fornés, V.; García, H. *Chem. Commun.* **2001**, 2546.
(7) Monk, J. A. *The Viologens: Physicochemical Properties, Synthesis and Applications of the Salts of 4,4-Bipyridine*; Wiley: New York, 1998.
(8) Bedioui, F.; Devynck, J.; Balkus, K. J., Jr. *J. Phys. Chem. B* **1996**, *100*, 8607.
(9) Senaratne, C.; Baker, M. D.; Zhang, J.; Bessel, C. A.; Rolison, D. R. *J. Phys. Chem. B* **1996**, *100*, 8610.
(10) Gemborys, H. A.; Shaw, B. R. *J. Electroanal. Chem.* **1986**, *208*, 95.
(11) Walcarius, A.; Lamberts, L.; Derouane, E. G. *Electrochim. Acta* **1993**, *38*, 2257.
(12) Walcarius, A.; Lamberts, L.; Derouane, E. G. *Electrochim. Acta* **1993**, *38*, 2267.
(13) Calzaferri, G.; Lanz, M.; Li, J.-W. *Chem. Commun.* **1995**, 1313.
(14) Hui, T.; Baker, M. D. *J. Phys. Chem. B* **2001**, *105*, 3204.
(15) Hui, T.; Baker, M. D. *J. Phys. Chem. B* **2002**, *106*, 827.
(16) Rolison, D. R. *Stud. Surf. Sci. Catal.* **1994**, *85*, 543.
(17) Dutta, P. K.; Ledney, M. *Prog. Inorg. Chem.* **1997**, *44*, 209.
(18) Doménech, A.; Formentín, P.; García, H.; Sabater, M. J. *J. Phys. Chem. B* **2002**, *106*, 574.
(19) Doménech, A.; García, H.; Alvaro, M.; Carbonell, E. *J. Phys. Chem. B* **2003**, *107*, 3040.
(20) Scholz, F.; Meyer, B. *Electroanalytical Chemistry, a series of advances*; Bard, A. J., Rubinstein, I., Eds.; Marcel Dekker: New York, 1998; Vol. 20, pp 1−87.
(21) Osteryoung, J.; O'Dea, J. J. In *Electroanalytical Chemistry*; Bard, A. J., Ed.; Marcel Dekker: New York, 1986; Vol. 14, p 209.
(22) Vetter, K. J. *Z. Elektrochem.* **1952**, *56*, 797.
(23) Laviron, E. J. *Electroanal. Chem.* **1984**, *164*, 213.
(24) Howell, J. O.; Wightman, R. M. *Anal. Chem.* **1984**, *56*, 524.
(25) Amatore, C.; Lefrou, C.; Pflüger, F. *J. Electroanal. Chem.* **1989**, *270*, 43.
(26) Garreau, D.; Hapiot, P. Savéant, J. M. *J. Electroanal. Chem.* **1990**, *289*, 73.
(27) Evans, D. H. *Chem. Rev.* **1990**, *90*, 739.
(28) Yoon, K. B. *Chem. Rev.* **1993**, *93*, 321.
(29) Beck, J. S.; Vartuli, J. C.; Roth, W. J.; Leonowicz, M. E.; Kresge, T. C.; Schmitt, K. D.; Chu, C. T.-W.; Olson, D. H.; Sheppard, E. W.; McCullen, S. B.; Higgins, J. B.; Schlenker, J. L. *J. Am. Chem. Soc.* **1992**, *114*, 10834.
(30) Bessel, C. A.; Rolison, D. R. *J. Phys. Chem. B* **1997**, *101*, 1148.
(31) Yoon, K. B.; Huh, T. J.; Kochi, J. K. *J. Phys. Chem.* **1995**, *99*, 7042.
(32) Bird, C. L.; Kuhn, A. T. *Chem. Soc. Rev.* **1981**, *10*, 49.
(33) Ashton, P. R.; Ballardini, R.; Balzani, V.; Credi, A.; Dress, K. R.; Ishow, E.; Kleverlaan, C. J.; Kocian, O.; Preece, J. A.; Spencer, N.; Stoddart, J. F.; Venturi, M.; Wenger, S. *Chem. Eur. J.* **2000**, *6*, 3558.
(34) O'Dea, J. J.; Osteryoung, J.; Osteryoung, R. A. *Anal. Chem.* **1981**, *53*, 695.
(35) Alvaro, M.; García, H.; García, S.; Márquez, F.; Scaiano, J. C. *J. Phys. Chem. B* **1997**, *101*, 3043.
(36) Kounaves, S. P.; O'Dea, J. J.; Chandresekhar, P.; Osteryoung, J. *Anal. Chem.* **1986**, *58*, 3199.
(37) Hawley, M. D.; Feldberg, S. W. *J. Phys. Chem.* **1966**, *70*, 3459.
(38) Feldberg, S. W. *J. Phys. Chem.* **1971**, *75*, 237.
(39) Amatore, C.; Savéant, J.-M. *J. Electroanal. Chem.* **1977**, *85*, 27.
(40) Amatore, C.; Savéant, J.-M. *J. Electroanal. Chem.* **1978**, *86*, 227.
(41) Amatore, C.; Savéant, J.-M. *J. Electroanal. Chem.* **1979**, *102*, 21.
(42) Zhang, J.; Lever, A. B. P.; Pietro, W. J. *Inorg. Chem.* **1994**, *33*, 1392.
(43) Andrieux, C. P.; Dumas-Bouchiat, J. M.; Saveant, J. M. *J. Electroanal. Chem.* **1982**, *131*, 1.
(44) Lei, Y.; Anson, F. C. *Inorg. Chem.* **1994**, *33*, 5003.
(45) Doherty, A. P.; Vos, J. G. *J. Chem. Soc., Faraday Trans.* **1992**, *88*, 2903.